

## Gauge fixing and extended Abelian monopoles in $SU(2)$ gauge theory in $2+1$ dimensions

G. I. Poulis

*TRIUMF, Theory Group, 4004 Wesbrook Mall, Vancouver, B.C. Canada V6T 2A3*

Howard D. Trottier

*Department of Physics, Simon Fraser University, Burnaby, B.C. Canada V5A 1S6*

R. M. Woloshyn

*TRIUMF, Theory Group, 4004 Wesbrook Mall, Vancouver, B.C. Canada V6T 2A3*

### Abstract

Extended Abelian monopoles are investigated in  $SU(2)$  lattice gauge theory in three dimensions. Monopoles are computed by Abelian projection in several gauges, including the maximal Abelian gauge. The number  $N_m$  of extended monopoles in a cube of size  $m^3$  (in lattice units) is defined as the number of elementary ( $1^3$ ) monopoles minus antimonopoles in the cube ( $m = 1, 2, \dots$ ). The distribution of  $1^3$  monopoles in the nonlocal maximal Abelian gauge is shown to be essentially random, while nonscaling of the density of  $1^3$  monopoles in some local gauges, which has been previously observed, is shown to be mainly due to strong short-distance correlations. The density of extended monopoles in local gauges is studied as a function of  $\beta$  for monopoles of fixed physical “size” ( $m/\beta = \text{fixed}$ ); the degree of scale violation is found to decrease substantially as the monopole size is increased. The possibility therefore remains that long distance properties of monopoles in local gauges may be relevant to continuum physics, such as confinement.

## I. INTRODUCTION

The dual Meissner effect was suggested as possible mechanism for confinement in non-Abelian gauge theories more than a decade ago by Mandelstam [1] and 't Hooft [2,3], and has recently been the subject of intensive lattice investigations [4–17]. In this picture of confinement, (color) magnetic monopoles are presumed to condense in the vacuum, forcing (color) electric fields between two sources to be squeezed into a flux tube. Magnetic monopoles are well understood to result in confinement in compact Quantum Electrodynamics, as has been demonstrated both analytically [18,19] and numerically [20,21]. The conjecture is that such “Abelian” degrees of freedom also drive confinement in nonAbelian theories. 't Hooft proposed that this mechanism can be realized in nonAbelian theories by imposing a gauge fixing condition that is invariant under a Cartan subgroup  $U(1)^{N-1}$  of the original  $SU(N)$  theory, referred to as an Abelian projection [3]. Singularities in the gauge-fixing condition are identified with monopole world lines in four dimensions ( $d = 4$ ) and monopole points (instantons) in three dimensions ( $d = 3$ ).

A lattice implementation of Abelian projection was formulated in Ref. [4,5], in which several gauge-fixing conditions were also developed (following 't Hooft [3]) that have been widely studied. The so-called maximal Abelian gauge is defined by gauge transformations  $G$  which maximize the following quantity [5] (we henceforth restrict our attention to  $SU(2)$ ):

$$R \equiv \sum_{x,\mu} \text{Tr} \left( \sigma_3 G(x) U(x, \hat{\mu}) G^\dagger(x + \hat{\mu}) \sigma_3 G(x) U^\dagger(x, \hat{\mu}) G^\dagger(x + \hat{\mu}) \right), \quad (1)$$

where  $U(x, \hat{\mu})$  are link variables. In the continuum limit,  $\max(R)$  reduces to the renormalizable differential gauge  $(\partial_\mu \pm ig A_\mu^3) A^{\pm,\mu} = 0$ , where  $A_\mu^\pm \equiv (A_\mu^1 \pm i A_\mu^2)/\sqrt{2}$ .

Local (generally nonrenormalizable) gauges can be defined by the diagonalization of an adjoint operator  $\Phi$  [4]:

$$\Phi(x) \rightarrow G(x) \Phi(x) G^\dagger(x) = \begin{pmatrix} e^{i\alpha(x)} & 0 \\ 0 & e^{-i\alpha(x)} \end{pmatrix}. \quad (2)$$

Examples of Eq. (2) are diagonalization of a plaquette or a Polyakov line [4]. We will refer to a gauge as “local” when the gauge condition can be imposed on a site-by-site basis.

Notice that Eqs. (1) and (2) are invariant under a local  $U(1)$  transformation  $G \rightarrow dG$ , where  $d$  is a diagonal matrix  $d = \cos \theta + i \sigma_3 \sin \theta$  [22]. The Abelian projection of a link  $U$  is defined, after gauge-fixing, as its component  $u$  in the corresponding subspace [4,5]

$$G(x) U(x, \hat{\mu}) G^\dagger(x + \hat{\mu}) \equiv w(x, \hat{\mu}) u(x, \hat{\mu}), \quad \text{Tr}(\sigma_3 w) \equiv 0 \quad (3)$$

( $w^\dagger w \equiv u^\dagger u \equiv 1$ ). The Abelian projection  $u(x, \hat{\mu})$  can be written as  $u(x, \hat{\mu}) = \exp[i\sigma_3 \phi(x, \hat{\mu})]$ . Monopoles are defined from the phases  $\phi$  (as described in Sec. II) and are associated with singularities in the gauge fixing which, in the context of Eq. (2), occur at points where  $\alpha(x) = 0$  [3].

One of the main issues that has been addressed in lattice investigations is whether the Abelian monopole density in a particular gauge exhibits scaling (thus having a well defined continuum limit).  $SU(2)$  lattice simulations in maximal Abelian gauge show scaling behavior for monopoles defined on elementary cubes of the lattice in  $d = 3$  [12], and there is some

evidence for scaling in  $d = 4$  [9,10]. On the other hand, it has been well established that the density of elementary monopoles in a variety of local gauges does *not* scale (this includes diagonalization of a plaquette and the Polyakov loop) [10].

As a result, the maximal Abelian gauge has become widely regarded as the only known gauge which may yet establish the role (if any) of Abelian monopoles in confinement. However, there is as yet no compelling reason why the degrees of freedom responsible for confinement in a gauge-invariant theory should only be manifest in this particular gauge. In fact, some monopole operators have recently been constructed which show evidence in local gauges for a spontaneous symmetry breaking that is correlated with the deconfinement phase transition [16,17].

We reconsider the lattice scale dependence of the monopole density in local gauges by analyzing the properties of *extended* monopoles. We work in three-dimensional SU(2) lattice gauge theory. The number  $N_m$  of extended monopoles in a cube of size  $m^3$  (in lattice units) is defined as the number of elementary ( $1^3$ ) monopoles minus antimonopoles in the cube ( $m = 1, 2, \dots$ ). A physical reason for studying extended monopoles is that confinement occurs on some finite physical length scale. The nonscaling behavior that has been observed in some gauges for elementary monopoles might therefore not be a good criterion for ruling out contact with the physics relevant to confinement.

Indeed, we find that nonscaling of the monopole density in some local gauges is due mainly to short-distance monopole-antimonopole fluctuations, which diverge in number as the coupling  $\beta \rightarrow \infty$ . On the other hand, such fluctuations are essentially absent in the maximal Abelian gauge. This is reflected in our calculation of the average minimum separation between a monopole and the nearest neighboring antimonopole,  $\langle r_{\min} \rangle$ . In maximal Abelian gauge  $\langle r_{\min} \rangle$  scales with  $\beta$ , while it vanishes (in physical units) with increasing  $\beta$  in the local gauges that we considered. [The dimensionless quantity  $\beta = 4/(g^2 a)$ , where the coupling constant  $g$  has units of (mass) $^{1/2}$  in three dimensions. We work throughout in lattice units, where the spacing  $a \equiv 1$ .]

Correlations between elementary monopoles and antimonopoles as functions of their separation are also calculated. Strong short-distance correlations are found in local gauges. On the other hand, in maximal Abelian gauge the monopole distribution is essentially random (the monopoles form a “plasma”). We speculate that large short-distance fluctuations in the gauge fields lead to the divergence in the number of monopoles in local gauges, while in the maximal Abelian gauge, which is imposed in nonlocal way, these fluctuations are effectively smoothed out.

We then consider the density of extended monopoles. In local gauges the density is found to decrease rapidly as the monopole “size”  $m$  is increased, the rate of change being maximal for  $m$  near unity. This can again be understood as due to an averaging over short distance fluctuations (i.e., as an averaging of the charges of elementary monopole-antimonopole pairs over larger volumes). By contrast, the density varies slowly with  $m$  in maximal Abelian gauge. We also consider the density of extended monopoles of fixed physical “size” ( $m/\beta = \text{fixed}$ ), as a function of  $\beta$ . For a finite value of  $m/\beta$  the density of monopoles in a typical local gauge does not scale; however, we find that the degree of scaling violation decreases substantially as the physical monopole “size” increases.

These results support the argument that strong short-distance fluctuations in the gauge fields can be effectively averaged out by a nonlocal gauge condition, as in the maximal

Abelian gauge, or (to a large extent) by considering extended monopoles on sufficiently long length scales in local gauges.

The organization of the rest of this paper is as follows. In Sec. II the various gauge fixing schemes and observables considered in this work are described. Our results are presented in Sec. III, and in Sec. IV we give our conclusions.

## II. METHOD

Abelian projection was carried out in the maximal Abelian gauge and in a number of local gauges. The maximization of  $R$ , Eq. (1), which defines the maximal Abelian gauge must be implemented iteratively. Following Ref. [9] we repeatedly sweep through the lattice, maximizing  $R$  locally by solving for  $G(x)$  analytically at each site, keeping  $G(x + \hat{\mu})$  at neighboring sites fixed. These iterations are repeated until  $G$  at all sites becomes sufficiently close to the identity:

$$\max\{1 - \frac{1}{2}\text{Tr } G(x)\} \leq \delta \ll 1, \quad (4)$$

with  $\delta = O(10^{-7})$  used as a stopping criterion. Note that this iteration procedure is not guaranteed to reach the global maximum of  $R$  [9]. Moreover, the iteration procedure is not guaranteed to increase  $\text{Tr } G(x)$  monotonically over successive iterations; hence the stopping criterion Eq. (4) is ambiguous. As a result, in practice the monopole number is not uniquely defined in the maximal Abelian gauge. For example, two field configurations differing only by an SU(2) gauge transformation will not, in practice, necessarily lead to the same number of Abelian monopoles in an actual calculation in maximal Abelian gauge. The implementation of the maximal Abelian gauge fixing also dominates the computational cost of the simulation, due to the large number of iterations (typically 1000) required to satisfy Eq. (4).

A local gauge that we consider is a simple implementation of Eq. (2): diagonalization of the field strength tensor,  $\Phi = F_{12}$  (cf. Ref. [4]). Note that Abelian projection in this gauge has the property that a pure-gauge configuration (a gauge transformation of links equal to the identity) will in general lead to a nonzero monopole density. Furthermore, the monopole numbers extracted from gauge-equivalent configurations in this gauge will not be equal in general. Calculations were also carried out in gauges defined by the diagonalization of rectangular Wilson loops of various sizes, as well as in an “unfixed” gauge (defined by  $\Phi = 1$  in Eq. (2)). These calculations lead to the same conclusions as drawn from the results presented here for  $\Phi = F_{12}$ .

Following Ref. [4] we compute phases of the Abelian projections of the gauge-fixed links  $u(x, \mu) \equiv u_0(x, \mu) + i\vec{\sigma} \cdot \vec{u}(x, \mu)$  (cf. Eq. (3)):

$$\phi(x, \hat{\mu}) = \tan^{-1} \left[ \frac{u_3(x, \hat{\mu})}{u_0(x, \hat{\mu})} \right], \quad \phi(x, \hat{\mu}) \in (-\pi, +\pi]. \quad (5)$$

Reduced plaquette angles  $\tilde{\phi}$  are then defined according to [20]:

$$\tilde{\phi} \equiv \phi - 2\pi N_s, \quad \tilde{\phi} \in (-\pi, +\pi], \quad (6)$$

where  $N_s$  is identified with the number of Dirac strings passing through the plaquette ( $N_s \in [-2, 2]$ ). The number of “elementary” monopoles  $N_{m=1}$  contained in a cube of size  $1^3$  is equal to the sum of Dirac strings  $N_s$  passing through the oriented  $1 \times 1$  plaquettes on the surfaces of the cube.

We define the number of extended monopoles  $N_m$  in a cube of size  $m^3$  as the number of elementary monopoles minus antimonopoles in the cube. The density  $\rho_m$  of extended monopoles of “size”  $m$  is given by

$$\rho_m = \frac{1}{2L^3} \sum_{i=1}^{(L/m)^3} |N_m(x_i)|, \quad (7)$$

where  $x_i$  labels the coordinates of the cubes of size  $m^3$ . We take  $m$  to divide the lattice length  $L$  (although this requirement can be relaxed); hence the total number of extended monopoles on the lattice vanishes.

The definition of  $N_m$  above corresponds to “type-II” extended monopoles defined in Ref. [7]; a “type-I” extended monopole number was also defined, which is computed from the phases of  $m \times m$  plaquettes on the surface of a cube of size  $m^3$  (using a suitable generalization of Eq. (6)). In an earlier version of this work we considered type-I extended monopoles. However, for large  $m$  the number of type-I monopoles approaches the strong coupling limit, since the phases of the  $m \times m$  plaquettes become essentially random [23,24]. Since we are interested in weak coupling continuum physics we consider only type-II monopoles in the rest of this paper.

The simulations were done mainly on a  $24^3$  lattice, using a bath algorithm at several values of  $\beta$  in the scaling region. The string tension on lattices of this size is found to scale for  $\beta \gtrsim 6$  (see, e.g., Ref. [25]). Some data was also taken at smaller values of  $\beta$  for comparison. We find that finite volume effects on the  $24^3$  lattice, as measured by the expectation value of the Polyakov line, become noticeable for  $\beta \gtrsim 12$  (which is the largest value in our data). Measurements were made on an ensemble of 500 configurations each separated by 100 updates, which is significantly longer than the autocorrelation time for any observable that we considered (the maximal Abelian gauge exhibits the longest autocorrelation time of the various gauges). We also used 200 configurations on a  $36^3$  lattice to obtain some results at large  $m$  (these data are identified explicitly in the following).

### III. RESULTS

The density  $\rho_1$  of elementary ( $m = 1$ ) monopoles is shown in Fig. 1 in maximal Abelian gauge (cf. Eq. (1)) and  $F_{12}$ -gauge ( $\Phi = F_{12}$  in Eq. (2)). It is clear that only maximal Abelian gauge exhibits scaling in  $\rho_1$ , and that the difference between the two gauges becomes more pronounced as  $\beta$  is increased.

Notice that maximal Abelian gauge has far fewer monopoles than the local gauges. To help understand this difference it is instructive to look at the spatial distribution of monopoles and antimonopoles. This is done by counting the number of monopoles  $N(r_{\min})$  for which the nearest antimonopole is a distance  $r_{\min}$  away. The results are shown in Fig. 2 for the  $F_{12}$ -gauge. As expected with a relatively large number of monopoles and antimonopoles, there are many short distance pairs; in fact, most monopoles have an antimonopole in a

neighboring lattice cell. A natural question is whether the monopoles and antimonopoles are correlated. Some insight into this question is obtained by comparing the result of the lattice simulation with  $N(r_{\min})$  for a completely random distribution of monopoles and antimonopoles. This is also shown in Fig. 2. A random distribution leads to an  $N(r_{\min})$  which is much broader than that observed in  $F_{12}$ -gauge. This is indicative of a strong short-range correlation between the monopoles and antimonopoles in this gauge, with significant enhancement of nearest-neighbor pairs.

Figure 3 shows  $N(r_{\min})$  for the maximal Abelian gauge at  $\beta = 8$ . Here the number of monopoles with nearby antimonopoles is very small so statistical errors are large, but  $N(r_{\min})$  is roughly consistent with a random distribution. There certainly is no enhancement of pairs with small separations as in  $F_{12}$ -gauge.

Figure 4 shows the average value of the minimum separation of a monopole and anti-monopole  $\langle r_{\min} \rangle$  for the two gauges as function of the number of monopoles (corresponding to  $\beta$  in the range 5 to 12). Again, for comparison, the results expected for a completely random distribution are plotted. For monopoles in maximal Abelian gauge we find reasonable consistency with a random distribution (a monopole “plasma”) but in  $F_{12}$ -gauge significantly smaller values of  $\langle r_{\min} \rangle$  are observed.

If the monopole density scales and the distribution is random we certainly expect  $\langle r_{\min} \rangle$  to scale with  $\beta$ . This is shown in Fig. 5. For maximal Abelian gauge,  $\langle r_{\min} \rangle$  scales very well. In  $F_{12}$ -gauge  $\langle r_{\min} \rangle$  vanishes in physical units as  $\beta$  increases.

These results support the idea that the excess of monopoles found in local gauges relative to maximal Abelian gauge is due to highly-correlated short distance fluctuations. This is further illustrated by considering the density  $\rho_m$  of extended monopoles.

In Fig. 6 we compare the density  $\rho_m$  in the two gauges at  $\beta = 6$ . The density in maximal Abelian gauge decreases slowly with  $m$ ; the decrease becomes more pronounced for  $m$  around the value of  $\langle r_{\min} \rangle$  for  $1^3$  monopoles in that gauge. This is consistent with the fact that strong short-distance correlations are absent in maximal Abelian gauge, with  $1^3$  monopoles forming a plasma, distributed on a length scale of  $O(\langle r_{\min} \rangle)$ . By contrast, the density in  $F_{12}$ -gauge decreases rapidly with  $m$ , with the rate of change being maximal near  $m = 1$ .

Figure 7(a) shows that the density of extended monopoles of fixed physical “size” ( $m/\beta = \text{fixed}$ ) scales well in maximal Abelian gauge. In  $F_{12}$ -gauge the density does not scale for any finite value of  $m/\beta$ , as illustrated in Fig. 7(b). The density  $\rho\beta^3$  in physical units increases roughly linearly with  $\beta$  for fixed  $m/\beta$ . However, the degree of scale violation decreases substantially as the physical monopole “size” increases. This is made evident by a plot of the slope  $\Delta(\rho\beta^3)/\Delta\beta$  as a function of  $m/\beta$ , given in Fig. 8. This is again consistent with a cancellation of short-distance monopole-antimonopole fluctuations.

#### IV. CONCLUSIONS

The results presented here demonstrate that the nonscaling of the density of elementary ( $1^3$ ) monopoles in a variety of local gauges, which has been previously observed, is due in large part to strong short distance correlations in those gauges. The distribution of  $1^3$  monopoles in maximal Abelian gauge was shown to be essentially random. The degree of scale violation in the density of extended monopoles in local gauges was found to decrease

substantially as the monopole “size” is increased. Our results support the argument that strong short-distance fluctuations in the gauge fields can be effectively averaged out by a nonlocal gauge condition, as in the maximal Abelian gauge, or (to a large extent) by considering extended monopoles on sufficiently long physical length scales in local gauges. The possibility therefore remains that long distance properties of monopoles in local gauges may be relevant to continuum physics, such as confinement.

#### **ACKNOWLEDGMENTS**

We thank K. Yee for fruitful conversations. This work was supported in part by the Natural Sciences and Engineering Research Council of Canada.

## REFERENCES

- [1] S. Mandelstam, Phys. Rep. **23C**, 245 (1976); *Monopoles in Quantum Field Theory*, Proceedings of the Monopole Meeting, Trieste 1981, Eds. N. S. Craigie, P. Goddard and W. Nahm (World Scientific, Singapore, 1982).
- [2] G. t'Hooft, Proceedings of the EPS International Conference on High Energy Physics, Palermo 1975, Ed. A. Zichichi (Editrice Compositori, Bologna, 1976).
- [3] G. t'Hooft, Nucl. Phys. **B190**, 455 (1981).
- [4] A. S. Kronfeld, G. Schierholz and U.-J. Wiese, Nucl. Phys. **B293**, 461 (1987).
- [5] A. S. Kronfeld, M. L. Laursen, G. Schierholz, U.J. Wiese, Phys. Lett. **B198**, 516 (1987).
- [6] J. Greensite and J. Winchester, Phys. Rev. D **40**, 4167 (1989).
- [7] T.L. Ivanenko, A.V. Pochinsky and M.I. Polykarpov, Phys. Lett. **B252**, 631 (1990).
- [8] T. Suzuki and I. Yotsuyanagi, Phys. Rev. D **42**, 4257 (1990).
- [9] V. G. Bornyakov, E. M. Ilgenfritz, M. L. Laursen, V. K. Mitryushkin, M. Muller-Preussker, A.J. van der Sijs, A.M. Zadorozhnyi, Phys. Lett. **B261**, 116 (1991).
- [10] L. Del Debbio, A. Di Giacomo M. Maggiore, S. Olejnik, Phys. Lett. **B267**, 254 (1991).
- [11] S. Hioki, S. Kitahara, S. Kiura, Y. Matsubara, O. Miyamura, S. Ohno, T. Suzuki, Phys. Lett. **B272**, 326 (1991).
- [12] V.G. Bornyakov and R. Grygoryev, Nucl. Phys. B (Proc. Suppl.) **30**, 576 (1993).
- [13] T.L. Ivanenko, A.V. Pochinsky and M.I. Polykarpov, Phys. Lett. **B302**, 458 (1993).
- [14] V. Singh, D. Browne, and R. W. Haymaker, Phys. Lett. **B306**, 115 (1993); P. Cea and L. Cosmai, Nuovo Cim. **107A**, 541 (1994).
- [15] J. D. Stack, S. D. Nieman, and R. J. Wensley, preprint ILL-TH-94-14, 1994.
- [16] L. Del Debbio, A. Di Giacomo, G. Paffuti, and P. Pieri, preprint IFUP-TH-30-94, 1994.
- [17] See also T. Suzuki, S. Ilyar, Y. Matsubara, T. Okude, K. Yotsuji, preprint KANAZAWA-94-15, 1994.
- [18] A. M. Polyakov, Nucl. Phys. **B120**, 429 (1977).
- [19] T. Banks, R. Myerson and J. Kogut, Nucl. Phys. **B129**, 493 (1977).
- [20] T. A. DeGrand and D. Toussaint, Phys. Rev. D **22**, 2478 (1980).
- [21] A. Irback and C. Peterson, Phys. Rev. D **36**, 3804 (1987); R. J. Wensley and J. D. Stack, Phys. Rev. Lett. **63**, 1764 (1989). See also H. D. Trottier and R. M. Woloshyn, Phys. Rev. D **48**, 4450 (1993).
- [22] We observe that Eq. (1) is also invariant under a purely “off-diagonal” transformation  $G(x) \rightarrow N(x)G(x)$ , where  $N(x) = i[\cos \theta(x)\sigma_1 + \sin \theta(x)\sigma_2]$  and  $\theta$  is arbitrary. The local gauge condition Eq. (2) is invariant under  $G(x) \rightarrow \varphi(x)G(x)$ , where  $\varphi$  satisfies  $[\varphi(x), \Phi(x)] = 0$ .
- [23] A. Cappelli, Nucl. Phys. **B275**, 488 (1986).
- [24] K. Yee, preprint LSUHEP-010194, 1994. We thank K. Yee for bringing this argument to our attention.
- [25] R. D. Mawhinney, Phys. Rev. D **41**, 3209 (1990).

## FIGURES

FIG. 1. Density of elementary ( $m = 1$ ) monopoles  $\rho_1\beta^3$  in physical units as a function of  $\beta$  in the maximal Abelian gauge (full circles) and  $F_{12}$ -gauge (full triangles).

FIG. 2. The number of elementary monopoles  $N(r_{\min})$  versus  $r_{\min}$  at  $\beta = 8$  in  $F_{12}$ -gauge (full triangles). Also shown is  $N(r_{\min})$  for a completely random distribution (open circles).

FIG. 3. The number of elementary monopoles  $N(r_{\min})$  versus  $r_{\min}$  at  $\beta = 8$  in maximal Abelian gauge (full circles). Also shown is  $N(r_{\min})$  for a completely random distribution (open circles).

FIG. 4. The average minimum monopole–antimonopole separation  $\langle r_{\min} \rangle$  versus the number of  $m = 1$  monopoles  $N_1$  in maximal Abelian gauge (full circles) and  $F_{12}$ -gauge (full triangles). Also shown is  $\langle r_{\min} \rangle$  for a completely random distribution (solid line).

FIG. 5. The average minimum monopole–antimonopole separation  $\langle r_{\min} \rangle$  as a function of  $\beta$ , for  $m = 1$  monopoles in the maximal Abelian gauge (main figure) and in the  $F_{12}$ -gauge (inset). The solid line in the inset shows a fit  $\langle r_{\min} \rangle / \beta = c / \beta$  to the data in  $F_{12}$ -gauge.

FIG. 6. Extended monopole density  $\rho_m$  at  $\beta = 6$  as a function of the “size”  $m$  in the maximal Abelian gauge (full circles) and  $F_{12}$ -gauge (full triangles).

FIG. 7. Extended monopole density  $\rho$  as a function of  $\beta$ , for several fixed monopole “sizes” in physical units ( $m/\beta = \text{fixed}$ ), in (a) maximal Abelian gauge and (b)  $F_{12}$ -gauge. The results for  $F_{12}$  gauge are taken from a  $36^3$  lattice. Straight lines are shown in Fig. 7(b) to guide the eye.

FIG. 8. Slope  $\Delta(\rho\beta^3)/\Delta\beta$  of the extended monopole density in  $F_{12}$ -gauge, as a function of  $m/\beta$ . The slope is estimated from the data in Fig. 7(b) using the two highest available  $\beta$  values.

$$\rho_1 \beta^3$$

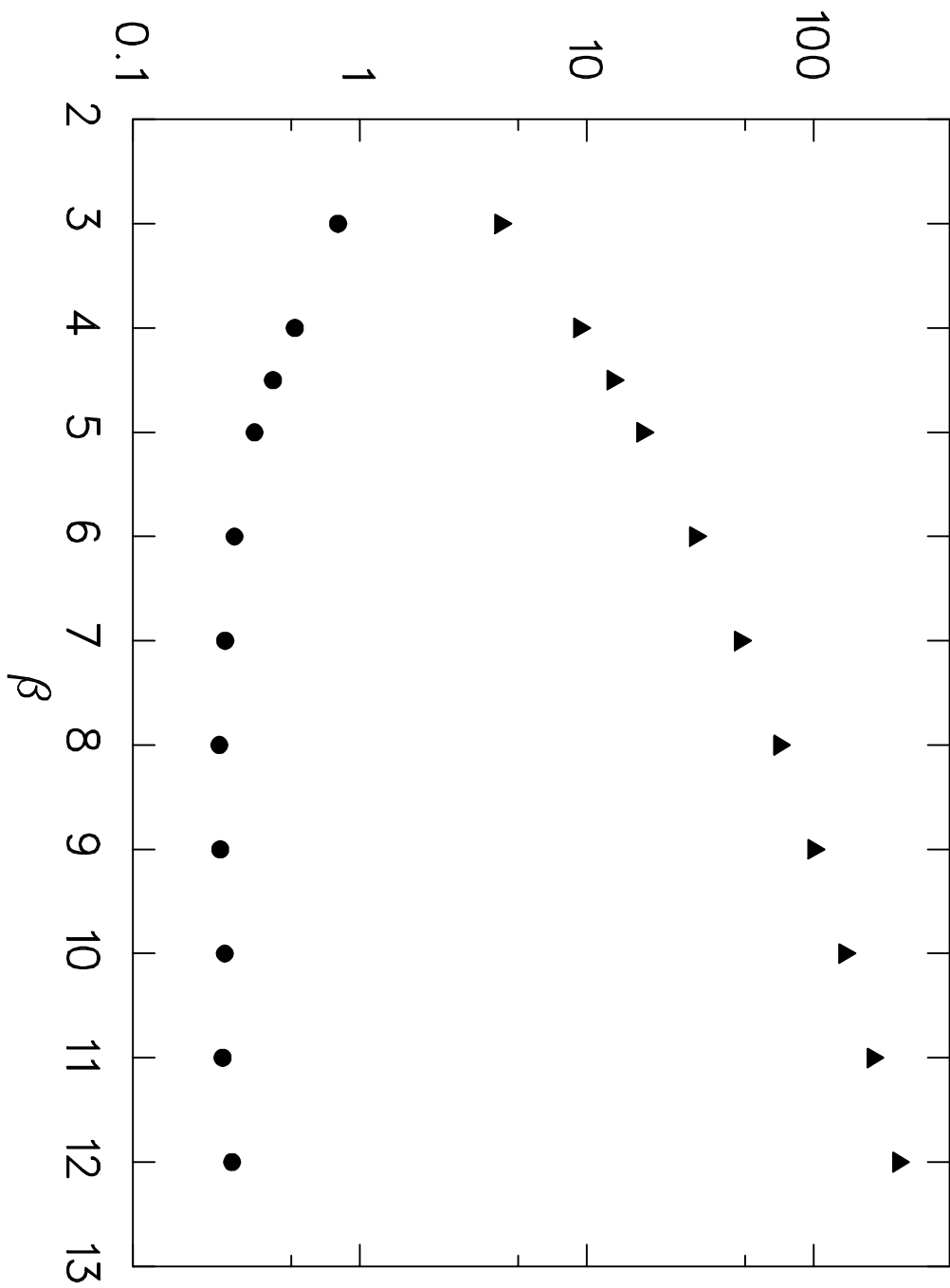


Fig. 1

This figure "fig1-1.png" is available in "png" format from:

<http://arxiv.org/ps/hep-lat/9312008v2>

This figure "fig2-1.png" is available in "png" format from:

<http://arxiv.org/ps/hep-lat/9312008v2>

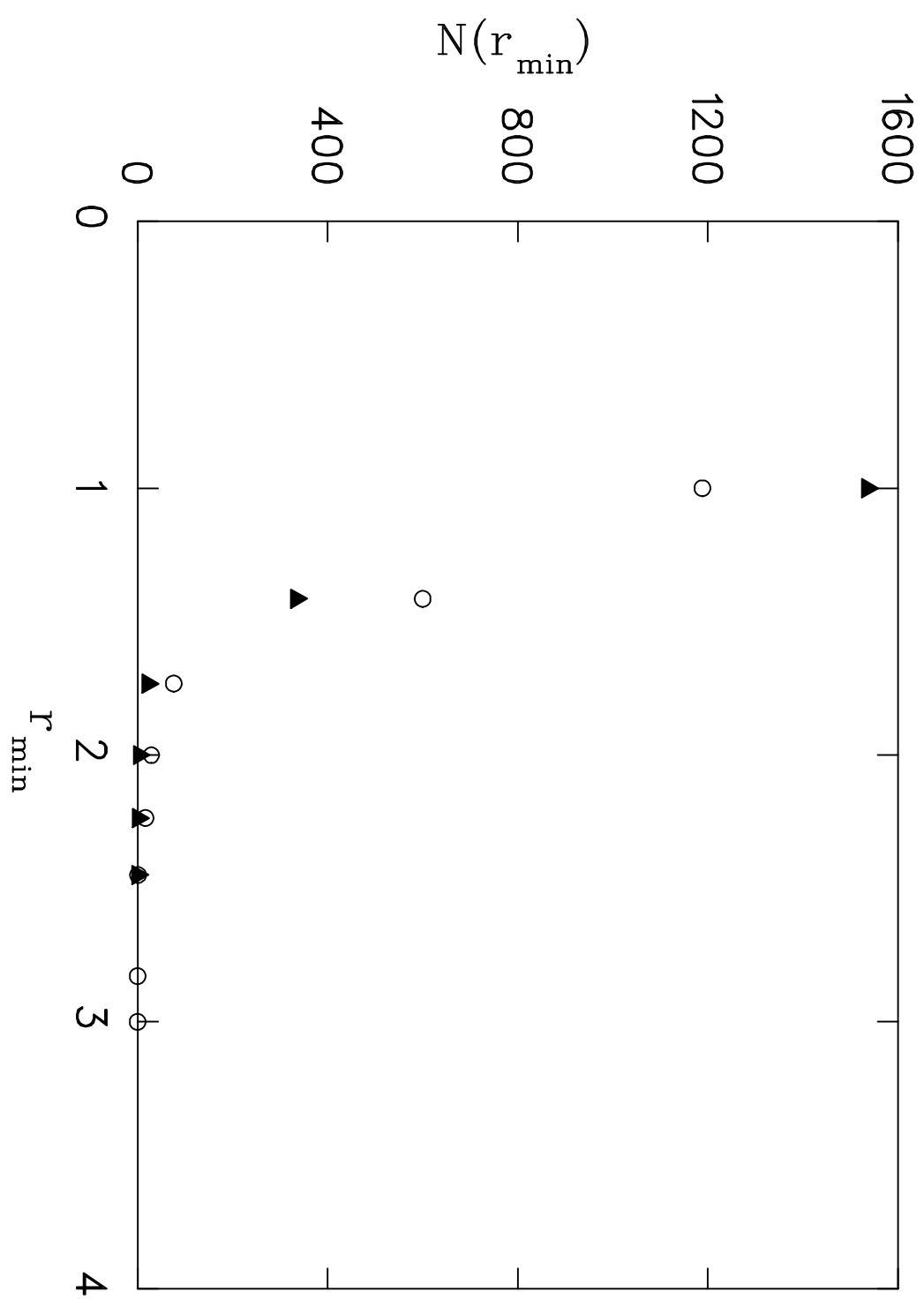


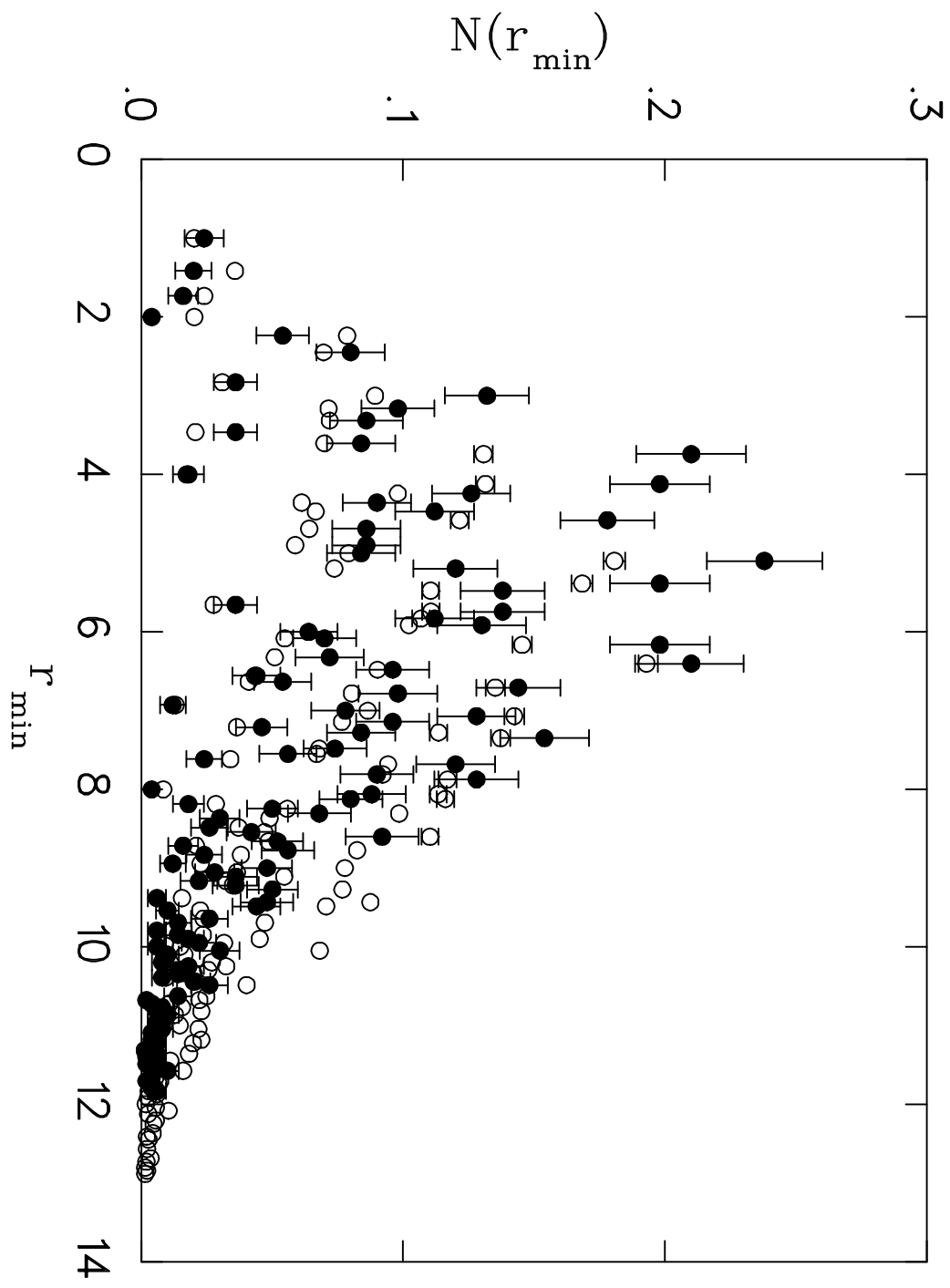
Fig. 2

This figure "fig1-2.png" is available in "png" format from:

<http://arxiv.org/ps/hep-lat/9312008v2>

This figure "fig2-2.png" is available in "png" format from:

<http://arxiv.org/ps/hep-lat/9312008v2>



This figure "fig1-3.png" is available in "png" format from:

<http://arxiv.org/ps/hep-lat/9312008v2>

This figure "fig2-3.png" is available in "png" format from:

<http://arxiv.org/ps/hep-lat/9312008v2>

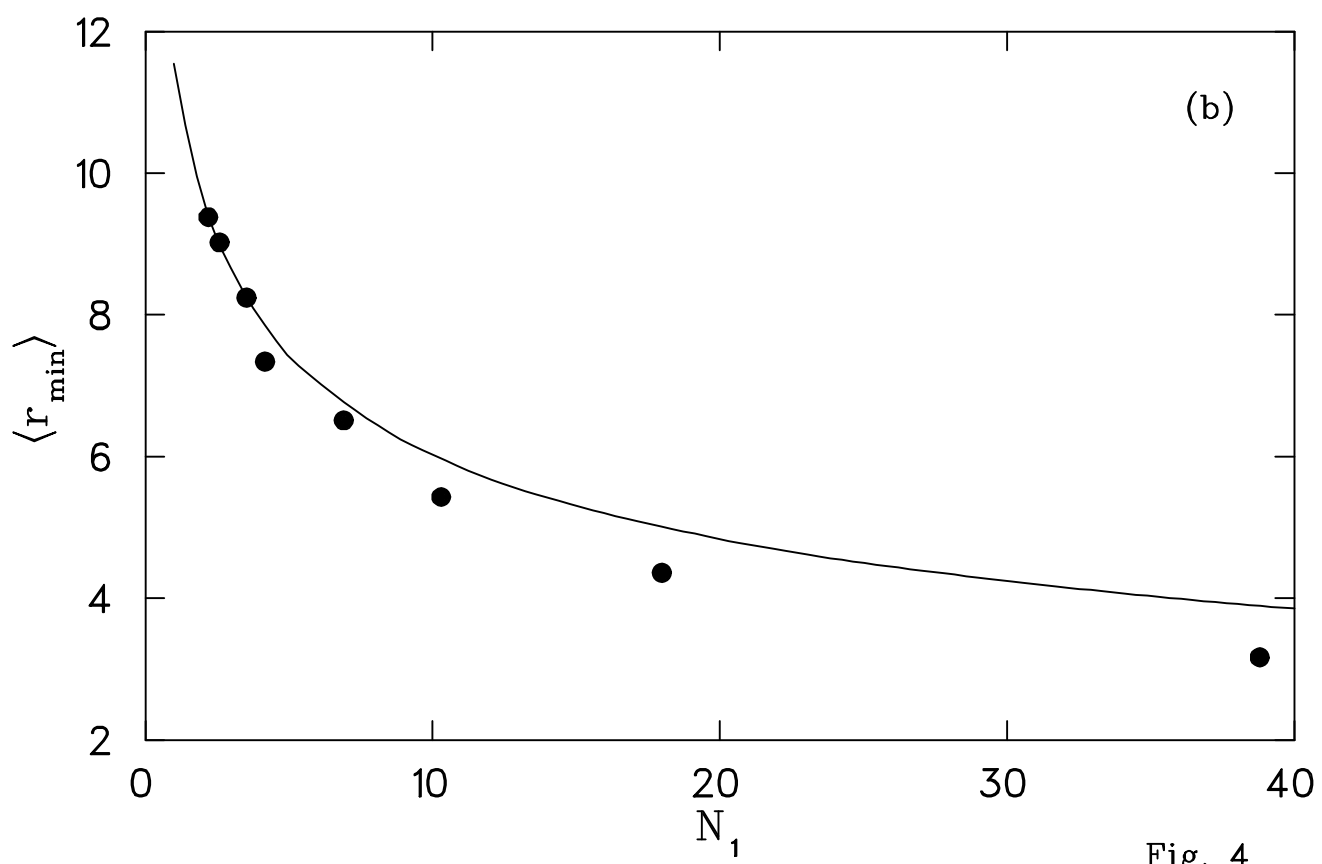
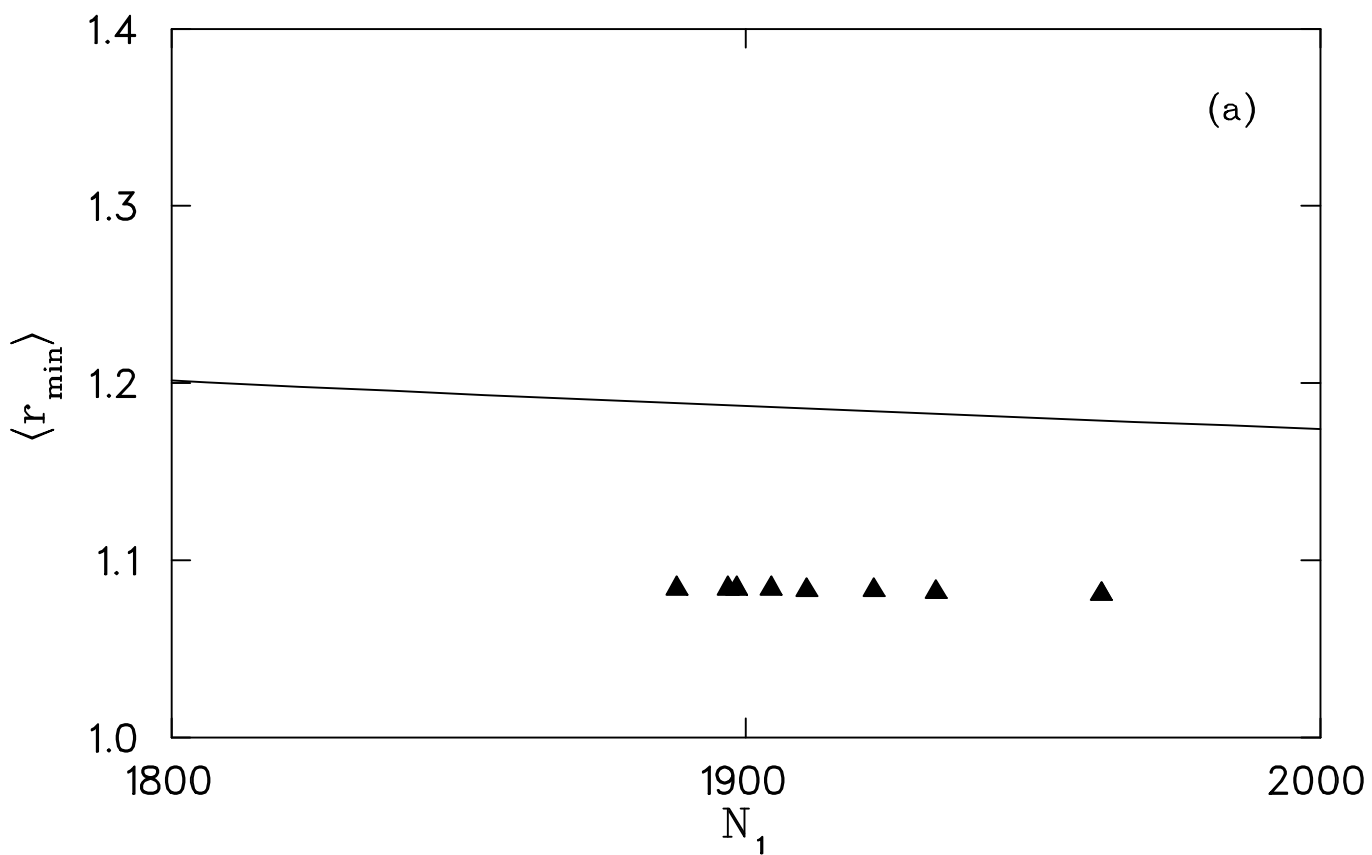


Fig. 4

This figure "fig1-4.png" is available in "png" format from:

<http://arxiv.org/ps/hep-lat/9312008v2>

This figure "fig2-4.png" is available in "png" format from:

<http://arxiv.org/ps/hep-lat/9312008v2>

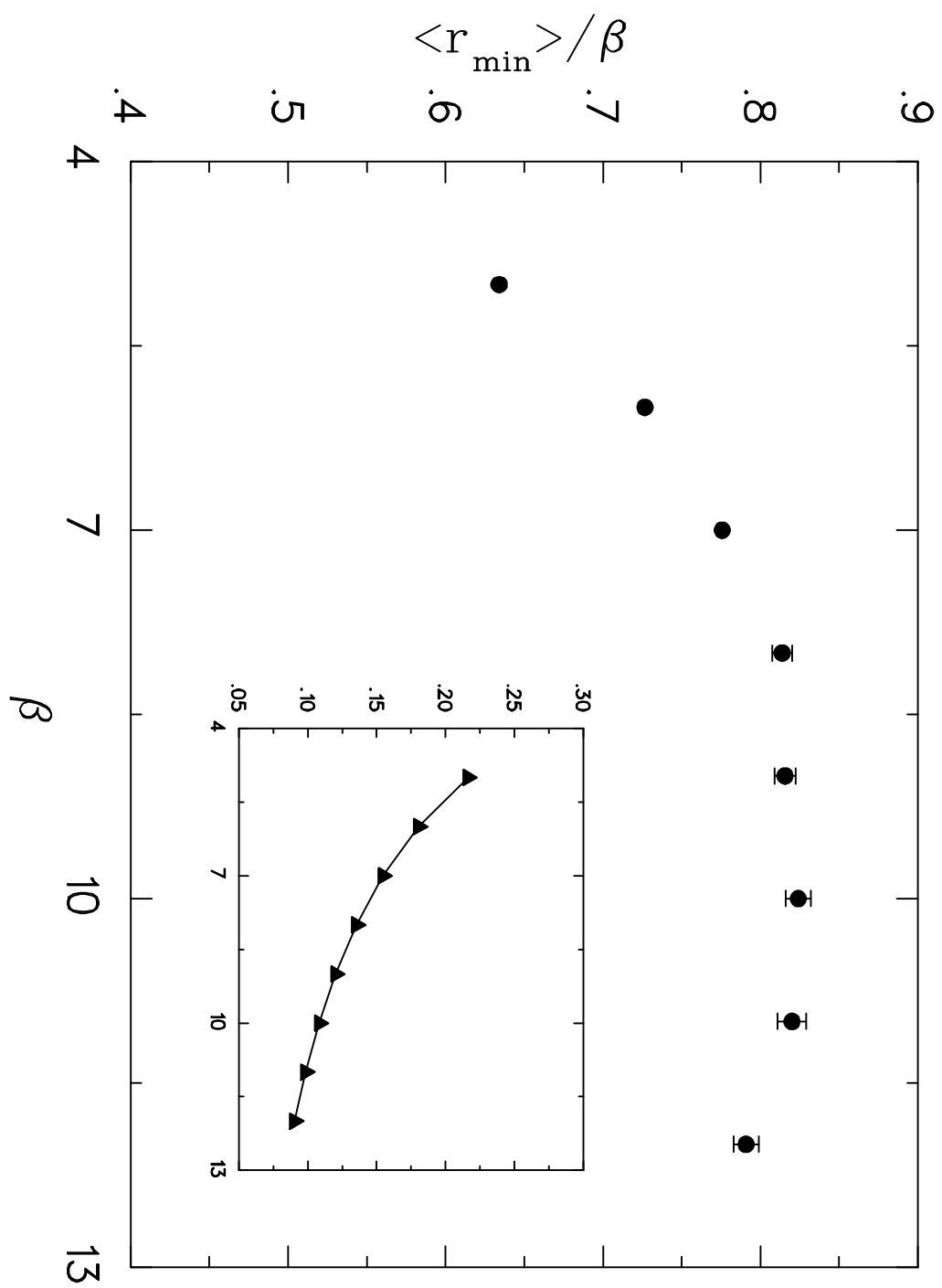
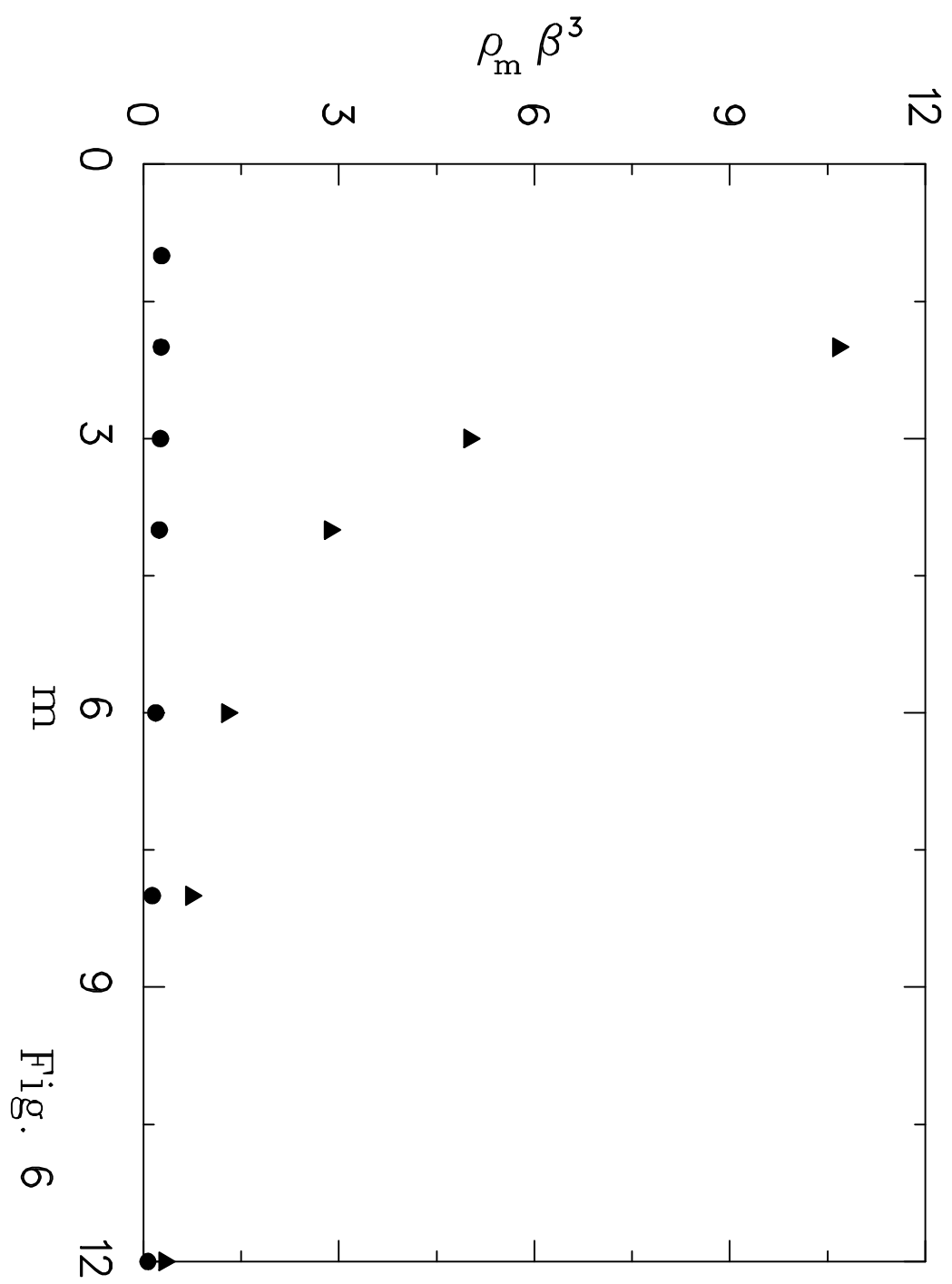


Fig. 5

This figure "fig1-5.png" is available in "png" format from:

<http://arxiv.org/ps/hep-lat/9312008v2>



This figure "fig1-6.png" is available in "png" format from:

<http://arxiv.org/ps/hep-lat/9312008v2>

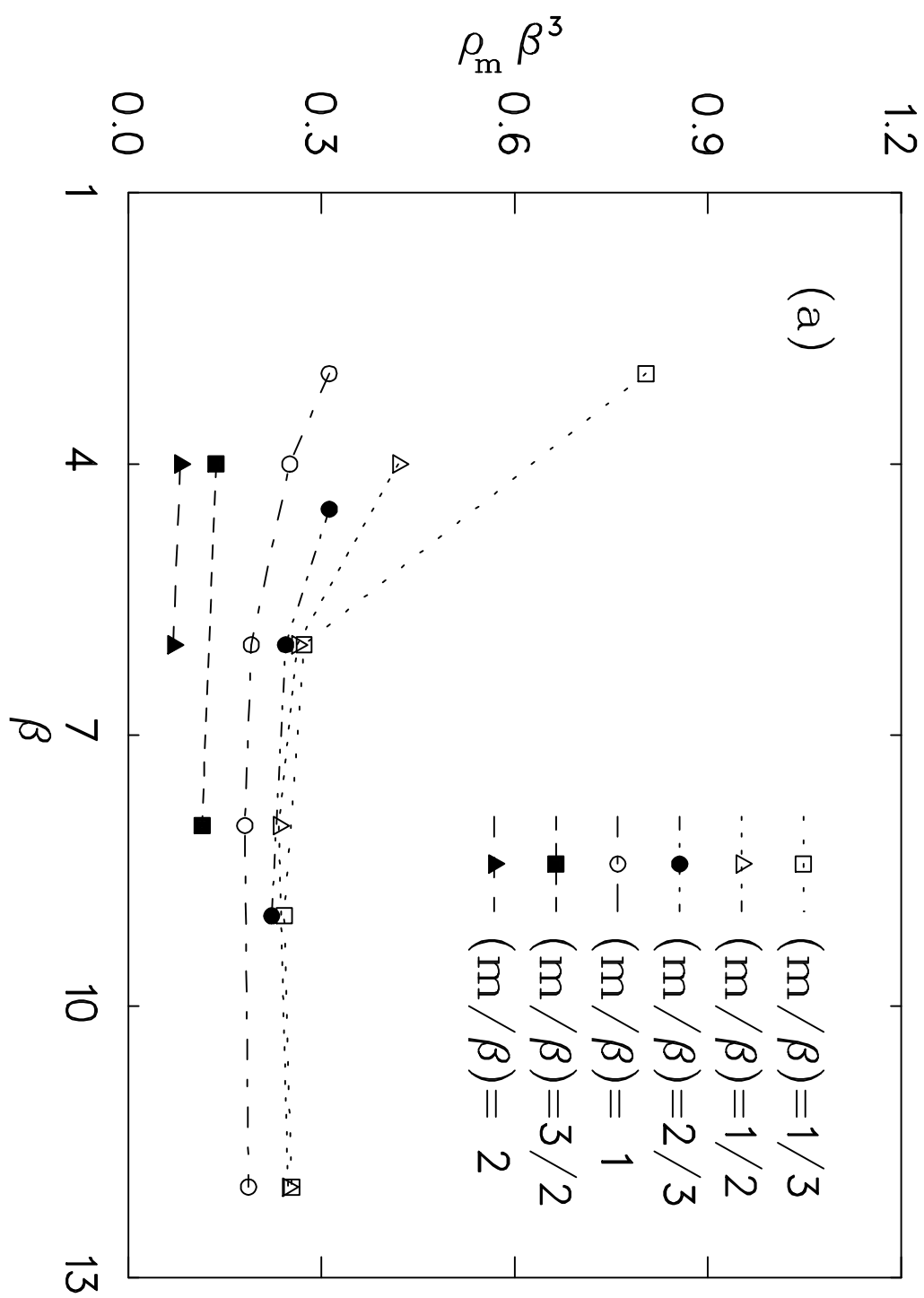


Fig. 7

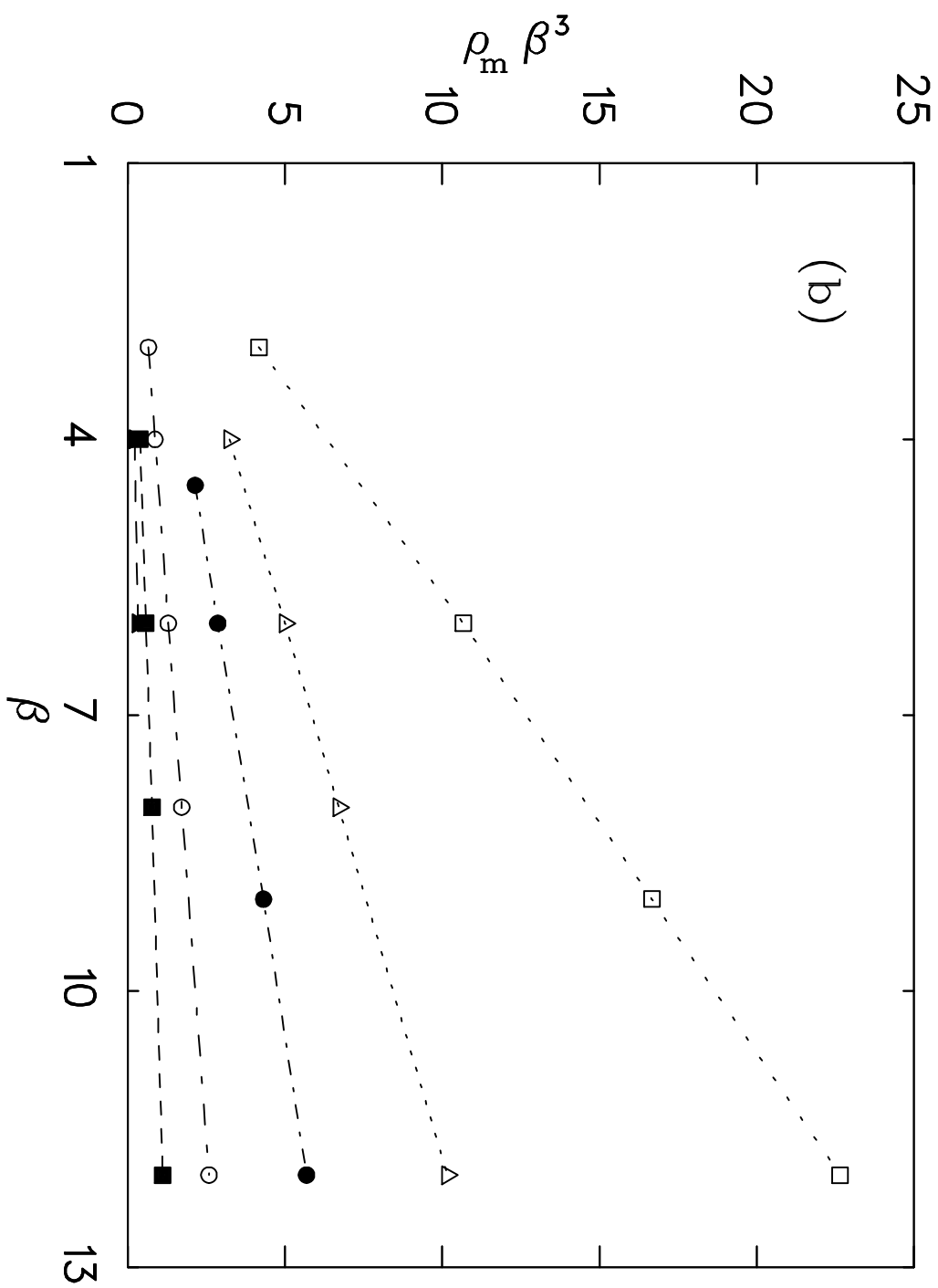


Fig. 7

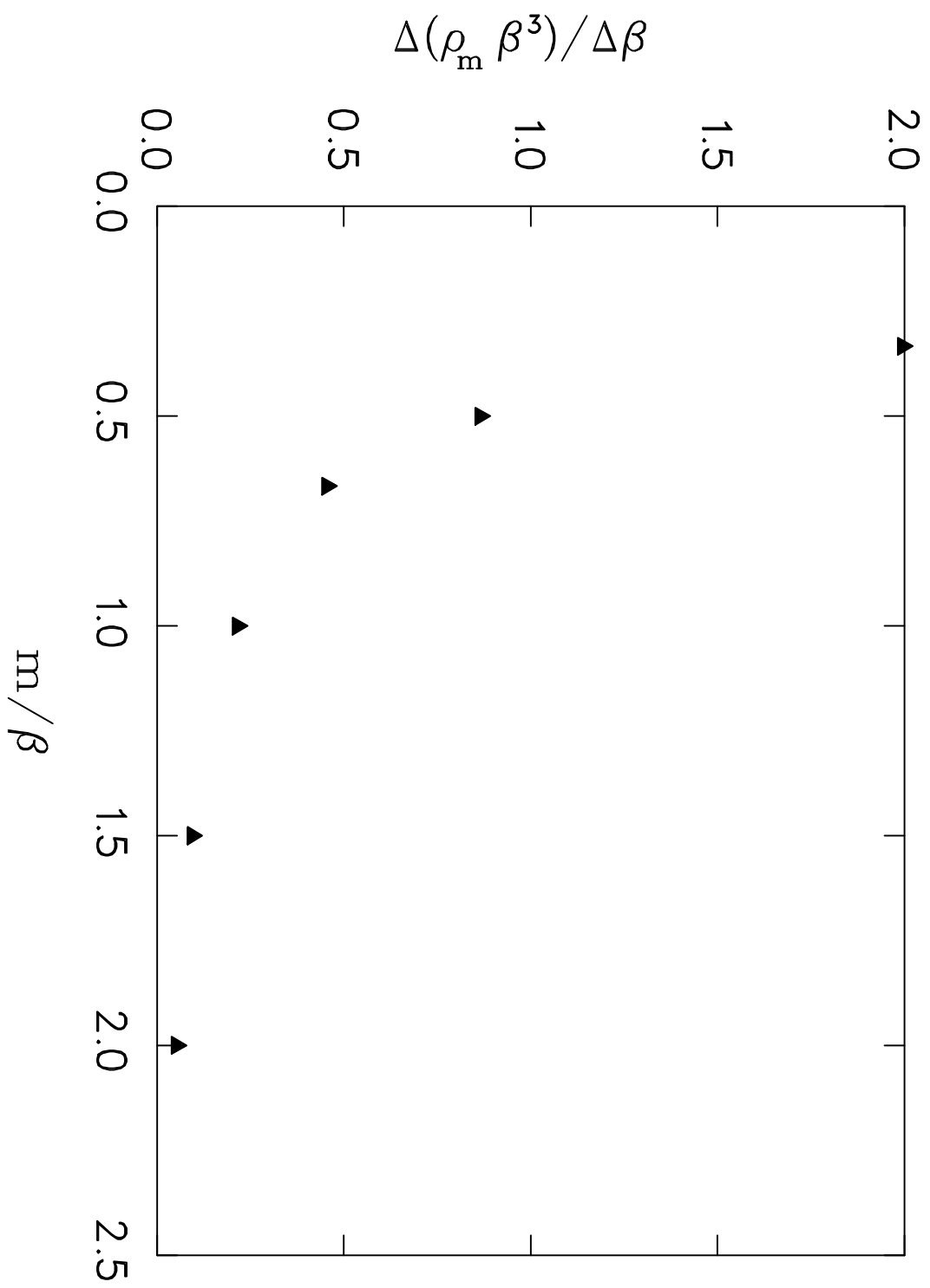


Fig. 8